Performance of High-Q Inductors in LTCC Using FTTF Techniques

Adam Paul Boutz and William B. Kuhn, *Senior Member, IEEE*

***Abstract*— Inductors have been produced in low-temperature co-fired ceramic in a manner that increases the cross-sectional area of the conductor. This geometry helps to compensate for high-frequency non-idealities, such as skin effect, current crowding and proximity effect. An array of various inductor geometries and probing structures has been fabricated and characterized. Qs of over 80 were confirmed, with Qs of over 100 believed to be possible. Accurate measurements of such values require careful consideration of error sources and the use of rigorous measurement techniques that are discussed. Finally, a filter has been fabricated to demonstrate the usefulness of these inductors in real-world applications.**

***Index Terms*— Full-tape-thickness-features, high-Q, inductors, low-temperature co-fired ceramic.**

I. Introduction

In the world of integrated circuits (ICs), on-chip inductors are something to be avoided. When they cannot be avoided completely, their use is minimized as much as possible or confined to limited applications. This is because integrated inductors consume valuable die area and traditionally had very low Qs due to thin metal traces and substrate-induced losses [1], [2]. This is a major problem for radio frequency ICs designers who require very high-Q inductors to make very sharp and clean filters. One solution to this problem is to move the inductors off-chip, using surface mount components, or embedded passives in substrates like low-temperature co-fired ceramic (LTCC). LTCC is often preferred for high performance applications, as an IC can be directly mounted on it while passive components and interconnects can be embedded on any number of layers.

Traditionally, inductors embedded in LTCC have taken the form of printed spiral traces of moderate thickness, and can, hypothetically, be of any size [3]. For the process used in this paper, traces are ~0.3 mil thick while all of the metal layers in an IC process combined may only be 0.1–0.2 mil thick. Hence, the Q of LTCC inductors can exceed that in radio frequency ICs. More importantly, LTCC components are free of the I^2R losses caused by currents in the semiconductor substrate that degrade the performance of on-chip components so strongly.

Despite these recognized benefits relative to on-chip inductors, there are still improvements that can be made on spiral LTCC inductors. The printed metal is still thin and 3-D inductor geometries can have performance advantages over planar ones. In [4] a solenoid was approximated by making turns of the inductor in multiple layers of the LTCC printed metal with vias connecting one turn to the next as shown in Fig. 1. Inductors of this type show improvements over planar spirals [3], but will still suffer from series resistance issues which are exacerbated by their small cross-sectional area. Increasing this area would increase Q.

Manuscript received June 26, 2009; revised May 24, 2010; accepted February 1, 2011. Date of publication July 22, 2011; date of current version August 12, 2011. Recommended for publication by Associate Editor R. Chanchani upon evaluation of reviewers' comments.

W. Kuhn is with the Department of Electrical and Computer Engineering, Kansas State University, Manhattan, KS 66506 USA (e-mail: wkuhn@ksu.edu).

A. P. Boutz was with the Department of Electrical and Computer Engineering, Kansas State University, Manhattan, KS 66506 USA. He is now with Lockheed Martin MS2, Eagan, MN 55121 USA (e-mail: adam.boutz@lmco.com).

Color versions of one or more of the figures in this paper are available online at http://ieeexplore.ieee.org.

Digital Object Identifier 10.1109/TCPMT.2011.2159717

II. Full-Tape-Thickness-Features (FTTF) Inductors

FTTF are metal conductors which occupy the entire thickness of a layer of LTCC green tape, rather than being sandwiched between the two layers [5], [6]. Trenches are cut into green tape in the same manner that vias are and then filled with metal. They can be formed by a large number of overlapping vias using either repeated punching operations or laser techniques.

A. Advantages Over Other Inductors

Forming inductors in this manner has several advantages. First, it increases the cross-sectional area of the conductor. This greatly decreases the DC resistance. Perhaps more importantly, it increases the surface area of the conductor in the regions where it is most important. In an isolated line, the skin depth in which current flow is concentrated at high frequency can be illustrated as shown in Fig. 2(a). Here, all four walls of the conductors carry current. Because of proximity effects [7], a solenoid can be considered to primarily conduct on the inside edge of each turn as in Fig. 2(b). Thus, inductors with traces built with FTTF techniques should yield lower resistance and higher Q than those constructed as shown in Fig. 1.

B. Fabrication Considerations

Special attention must be paid to the layout of these inductors. Because the elements span the thickness of the tape, they are 'open' to the layers above and below. This means that they can contact both flat metal printed onto the tape layer as well as other FTTF elements. Any features not intended to be electrically connected should not cross on adjacent layers. In the case of a coil, this means leaving a layer of tape between

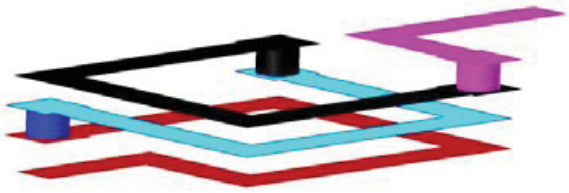

Fig. 1. Typical helical inductor made from thin metal traces.

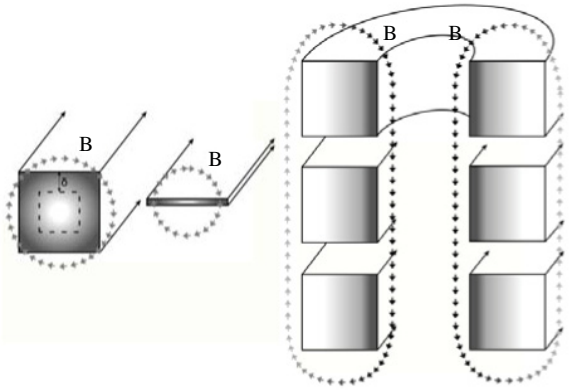

Fig. 2. Current distribution in (a) isolated lines and (b) coils.

turns. Also, the physical stability of the tape must be taken into consideration. To form a FTTF, a significant amount of green tape must be removed. Care must be taken so that a section of tape does not become isolated enough that it can no longer be supported. For instance, a uniform ring of FTTF cannot be fabricated because the tape that fills the center will fall out before the layer can be filled with metal paste and fired to make it rigid. Because the ceramic tape is very thin and flexible, while green, multiple points of support may be required to prevent a mostly isolated region from 'drooping' or 'sagging'. The exact limitations are dependent on the materials, process and geometries used.

1) Lasers Versus Punching: As previously stated, the fabrication process we employ uses overlapping via punches. A more common method of creating vias uses lasers. This can be applied to creating trenches as well. It is a much faster process and has the added benefit of not physically fatiguing the green tape due to repeated strikes by the punch. The equipment required, however, is more costly than the punching process. More importantly, laser cutting has other drawbacks which limit its usefulness in this particular application. The cuts which are made by the laser have rough sides, and the cuts do not have a consistent width for the entire cross-section of the tape [8]. Thus, we favor the punch method in the quest for the highest Q values possible.

C. Designs Examined

A large array of inductors was produced, but most of the more complicated varieties either underperformed or had fabrication problems. Presented in this paper are three of the simplest and most informative structures, consisting of a vertical solenoid, a vertical solenoid with a shield, and a planar spiral for reference.

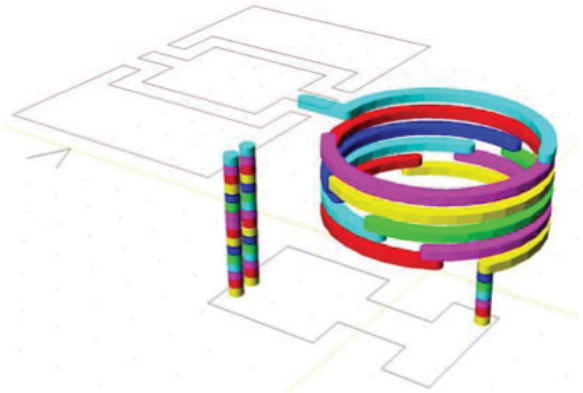

Fig. 3. Vertical solenoid.

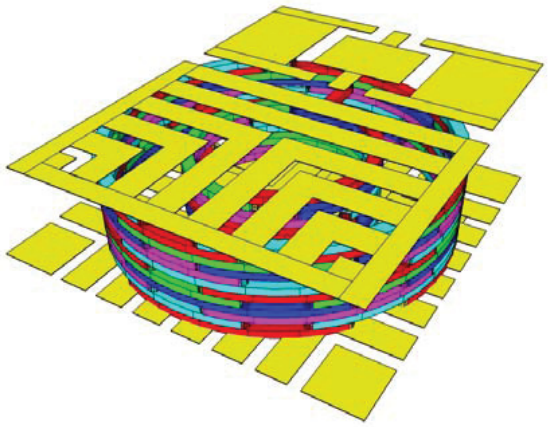

Fig. 4. Shielded vertical solenoid.

1) Vertical Solenoid: Vertical refers to the axis of the coil which is perpendicular to the plane of the green tape. The tape used is 4 mil thick and the punch size is 6 mil wide after firing. The diameter of the inductor is 80 mil. There is about half of a turn on each layer, with a total of 4.5 turns (see Fig. 3).

2) Shielded Vertical Solenoid: This structure is very similar to the first structure, except that this is entirely enclosed in a ground shield for extra isolation. This shield is also made of FTTFs for the round, coaxial portion. The ends are made of flat metal as shown in Fig. 4. They are patterned to help reduce eddy losses. Most of what is visible in Fig. 4 is the shield, but the inductor of Fig. 3 can be seen in the interior.

3) Planar Spiral: A two-turn planar spiral inductor was included to serve as a reference to compare with the 3-D FTTF inductors. The traces are about 10 mil wide and the inductor is 80 mil square, as shown in Fig. 5.

4) Spiral Stack: Finally, a multilayer inductor was also fabricated to provide a data point to demonstrate how an inductor with a similar inductance and footprint would behave if made using the traditional flat-metal technique. It consists of five planar spirals stacked in such a way that the current spirals both 'in' and 'out' are always maintaining a clockwise rotation. From above, this would appear very similar to Fig. 5. Fig. 6 shows this structure in profile, looking between the layers.

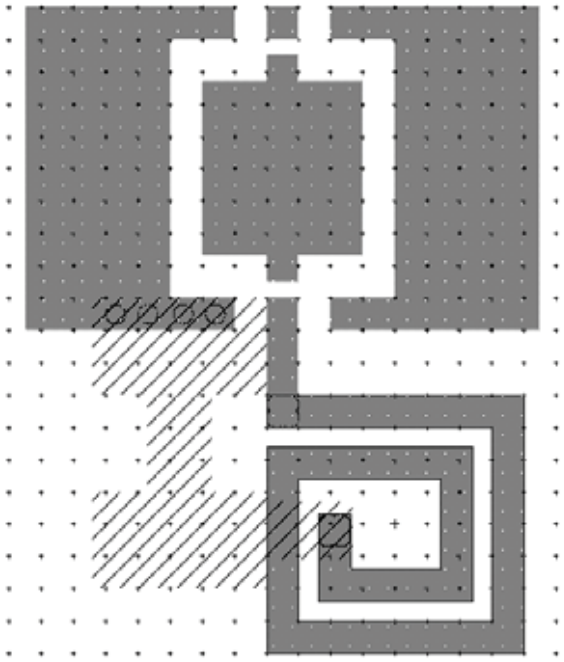

Fig. 5. Planar spiral.

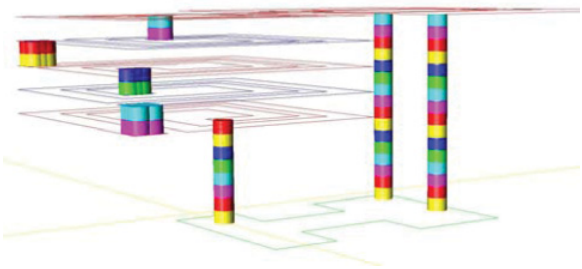

Fig. 6. Planar spiral.

5) Probing and Resonator Structures: In Figs. 5 and 6, additional features besides the spiral itself are clearly evident. On the top-side, where the spiral is patterned, rectangular pads are provided. These allow for the placement of parallel capacitors to form an LC resonator. On the back side (shown in cross-hatch), the "I" structure is provided to allow a series resonator to be formed. This is done by cutting the center of the "I" and soldering in a 0402 size SMD device. These pad locations for optional capacitors are used to help validate the very high Q values expected, as discussed in Section IV.

III. L and Q Estimations

Estimates of L were found from the Wheeler formula for single-layer solenoids [9]. The estimates for Q were based on first-order approximations and geometry. For the purposes of finding resistance, the conductor is assumed to be reduced to only the area carrying current as determined by one skin depth δ [10] on the inside of the coil as shown previously in Fig. 2. The inductor's series resistance R can then be estimated as

$$R = \frac{l_{path}}{\sigma A} \tag{1}$$

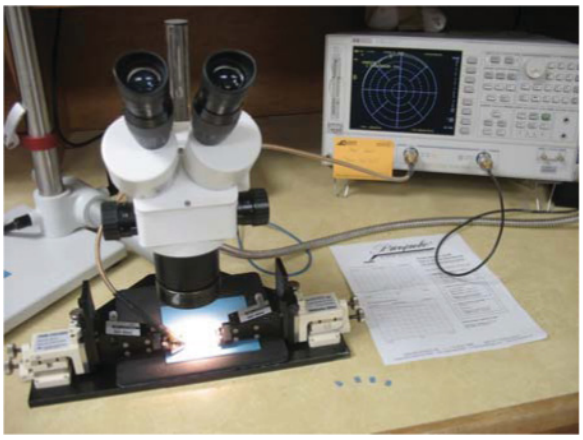

Fig. 7. Test setup.

where l_{path} is the total length of the inductor turns, σ is the metal volume conductivity and A is the cross-sectional area, through which current flows. The cross sectional area of the vertical inductors, A, can be approximated as

$$A \cong \delta h \tag{2}$$

where h is the thickness of the traces corresponding to the tape thickness, and δ is skin depth which is a function of frequency and the conductivity of the fired gold paste ($\sigma = 2.22E7$ s/m or 6.77E6 s/ft in our case). From the geometry of Fig. 4, the path length of the inductors is the distance the conductor would cover if it could be straightened

$$l = 2\pi r N. \tag{3}$$

The AC resistance of the coils can be found by substituting (2) and (3) into (1)

$$R \cong \frac{2\pi r N}{\delta h \sigma}. \tag{4}$$

Finally, the Q factor is found by the well-known equation

$$Q = \frac{2\pi f L}{R}.$$

Equations (1)–(5) use metric units. This does not account for the extra current-carrying area on the top and bottom turns and so the approximations can be considered conservative estimates. In addition, it should be noted that they only apply for frequencies where 2δ is less than the trace width. Based on these, the 80 mil diameter FTTF solenoids were estimated to have $L = 52$ nH and $Q(500\ \text{MHz}) = 59$.

IV. Measured Results

Measurements were taken with an HP8735E vector network analyzer (VNA) and GGB Industries ECP18-GSG-500-DP coplanar probes, as pictured in Fig. 7. The measurement system was calibrated using a GGB CS-9 calibration substrate.

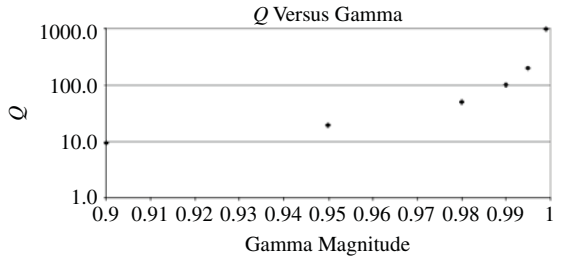

Fig. 8. Q versus Gamma for best case measurement ($\angle\Gamma = 90°$).

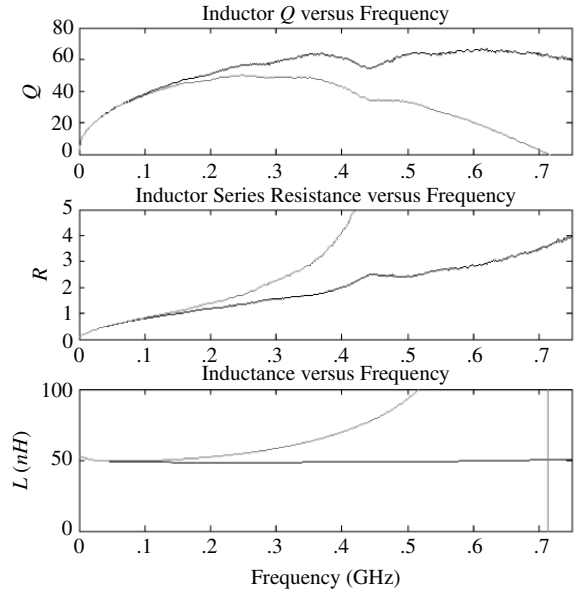

Fig. 9. Measured results for the vertical solenoid.

A. High-Q Measurement Techniques

It is difficult to take accurate measurements of high-Q inductors, and great care must be taken to avoid misleading results. To this end, the probing structure included with each inductor allows four types of measurements [11], [12]. The simplest of these is the VNA 1-Port method. This is a simple S11 measurement of the reflection coefficient, Γ. It is a widely used method of measuring Q, but it has serious limitations for Q values of about 50 or higher [12]. As Q becomes large, $|\Gamma|$ quickly approaches 1. Using the classic definition of Q, it can be shown that the network analyzer's measurements will be most accurate in the region near $\Gamma = +j$. Q as a function of Γ in this region of the Smith chart is plotted in Fig. 8. From this graph, it is clear that an accuracy of better than 1% is required to measure a Q of 100. For example, if a gamma magnitude accuracy of 0.5% is assumed (about $2\times$ better than manufacturer's stated performance), an inductor measurement showing a reflection coefficient of $+0.99\ j$ on the display can imply a Q anywhere from 66 to 200 [12]. Thus a typical VNA does not have the accuracy required to measure the Qs we believe are possible.

Several resonance-based methods are possible to address this accuracy issue. One method places a capacitor in series with the inductor to form a resonator. The series RLC circuit can then be measured for center frequency and bandwidth

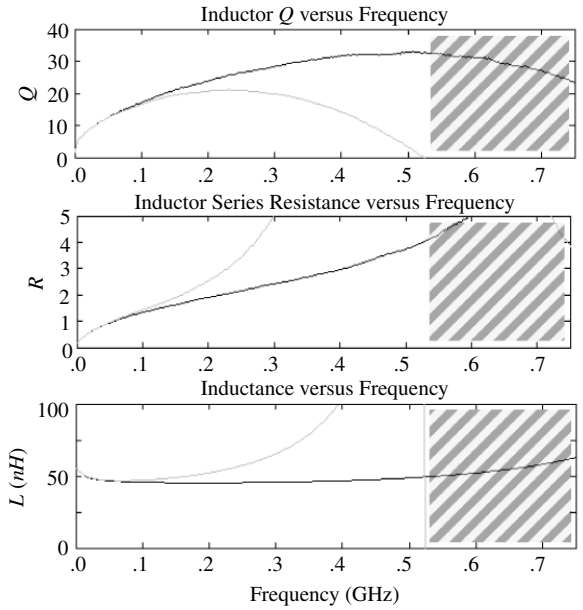

Fig. 10. Measured results for the shielded vertical solenoid. Frequencies above self resonance are shaded (see text).

and the resonator Q can be found directly from those. The main drawback to this method is that it can only be applied to a single frequency at a time, unlike the VNA 1-Port method which can measure a large number of frequencies at a time. Also, it requires external capacitors and bulky pads to place them on. A related technique attempted in this research used parallel resonating capacitors, but suffers from similar limitations. Thus, most measurements reported below use the standard VNA 1-port technique. The resonance technique was used primarily to validate Q measurements at selected frequencies.

B. VNA 1-Port Measurements

Graphs of Q, series resistance and inductance versus frequency for the four test inductors are shown in Figs. 9–12. Each graph contains two curves, representing two definitions for Q. The commonly accepted formula for Q is X/R. However, this is not an entirely accurate form for many applications. By this definition Q goes to 0 at an inductor's self-resonant-frequency. The true definition of Q is peak energy stored divided by the energy dissipated per cycle. For applications such as filter design, this definition provides a more useful assessment of the performance the inductor can achieve in an application [1]. To properly present our results, therefore, the plots have two curves. The gray line represents the conventional definitions of Q, R, and L. The black line is the same data, but the admittance of the internal capacitance has been mathematically removed to give a realistic estimate of the true Q value.

It should be noted that the results here are only valid until the self-resonant frequency of an inductor, indicated by an asymptote in the uncompensated 'L' value. Above this frequency, the structure is capacitive and the definition of 'Q' no longer holds true. This is the reason that part of Fig. 10 is shaded out.

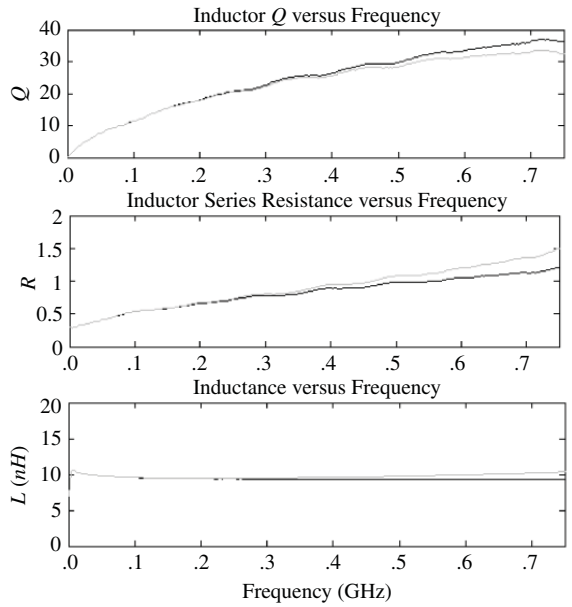

Fig. 11. Measured results for the planar spiral.

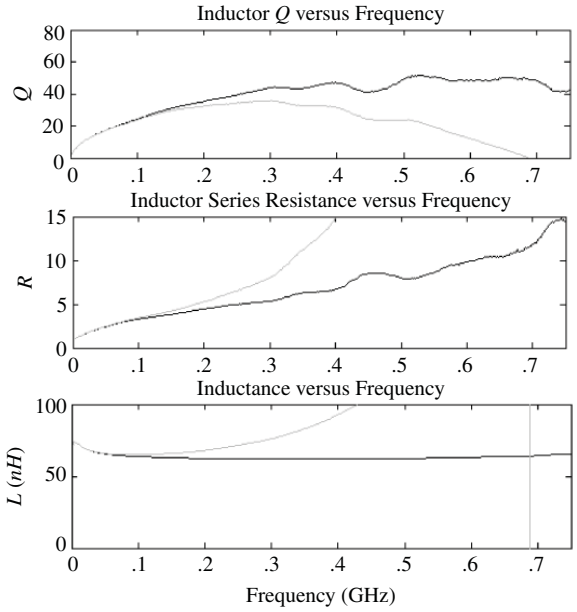

Fig. 12. Measured results for the spiral stack.

C. Resonant Q Measurement

As discussed in Section IV-A, Q values above about 50 are not measured with sufficient accuracy when using a network analyzer in a simple S11 measurement mode. High-Q RF capacitors were therefore soldered to the included pads of the high-Q FTTF inductors, allowing measurements of bandwidth to be taken at their resonance frequencies, from which the Q can be found. The resulting Q values are shown in Table I.

These values of Q are about 10% to 20% higher than those taken with the S11 method and are believed to be more accurate. However, even these measurements should be refined. The source and load impedances of the VNA load down the circuit and widen the bandwidth. Nevertheless, the values in Table I are believed to be good lower-bounds on the true inductor Q values. Both the simple S11 measurements and the more involved single-frequency resonant Q measurements confirm that the FTTF inductors offer substantial Q improvements over the simple planar metal design.

TABLE I
RESONANCE MEASUREMENTS OF FTTF VARIANTS

	f_0	Q
Vert Sol.	287 MHz	65.5
	445 MHz	75.2
Shielded Vert Sol.	227 MHz	25.4
	–	–

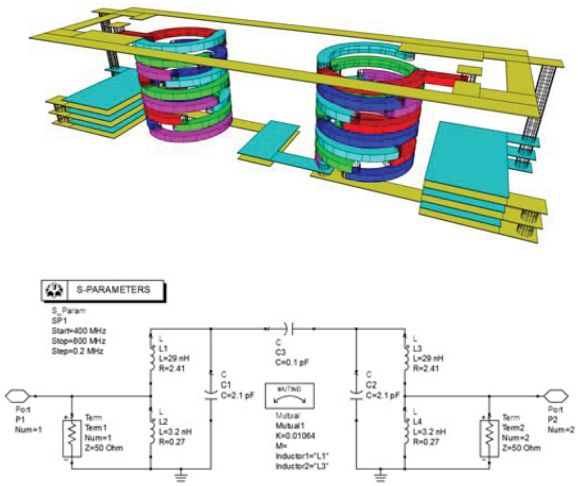

Fig. 13. 2-Pole filter: perspective view and simulated circuit.

V. POTENTIAL APPLICATIONS

A. 2-Pole Filter

To demonstrate the application of high-Q FTTF inductors, a prototype 2-pole filter was fabricated with the array. This filter uses two smaller 40 mil diameter coils with magnetic and capacitive coupling to provide a narrow bandwidth response in a small footprint. The filter shown in Fig. 13 uses flat metal capacitors as well as FTTF inductors and requires no components external to the LTCC, and so is ideal for use with interfacing to an IC.

The inductor was simulated as in Fig. 14 and then measured. The filter was designed with some tunability (each cap had a plate on an outer layer which can be scribed away). Due to a larger-than-expected capacitance between the coils, the system was initially over-coupled. The removal of the center coupling cap improved the response. A small amount of trimming on one resonator cap was also required to bring these into alignment. The final result can be seen in Fig. 15. The filter bandwidth is approximately 30 MHz at a center frequency of approximately 600 MHz, giving a selectivity Q of 20. Refinement of the simulation model using the measured response and insertion loss suggests that the Q values of the inductors are in the range of 50, which is consistent with the range of Qs seen in the direct measurements of the inductors

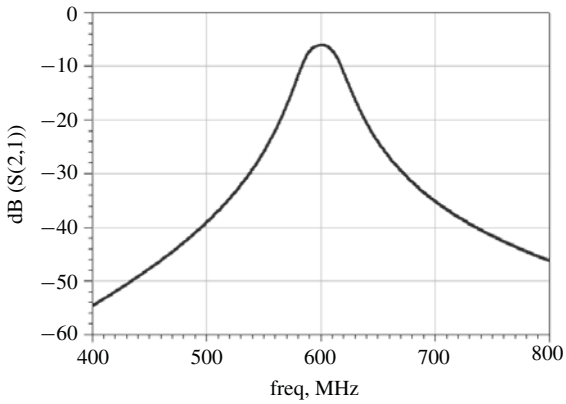

Fig. 14. Filter simulation.

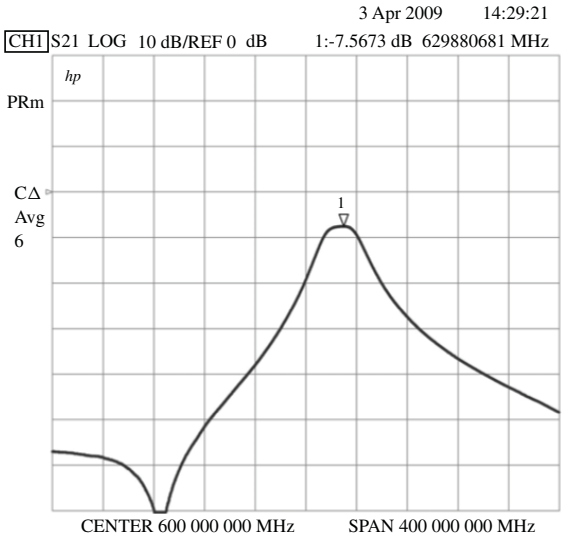

Fig. 15. Measured filter response. Center frequency of display is 600 MHz and span is 400 MHz.

used (but are somewhat lower Q than the best spiral of Figs. 3 and 9 due to the smaller size).

The inductors in this filter are tapped very near ground to provide a 50 Ω impedance to match the VNA. It would be a simple matter to design the filter to match the kinds of impedances that would be seen on-chip, making the bondwire or flip-chip transition between filter and circuit easier.

B. Deep Loop Resonator

Finally, an attempt was made to reach even higher Q values by significantly increasing the height term in (2) and resonating with an embedded capacitor. The resulting deep loop resonator pictured in Fig. 16 is descriptively named. It is an 80-mil diameter, single-turn inductor with a vertical axis which is 15 tape layers thick. Interspersed between the ends of the loop are the plates of the capacitor, forming a parallel LC resonator. The plates are separated by the same ceramic that supports all the other features; Dupont 951 Green Tape forms the dielectric.

The estimations applied to the other inductors suggest a Q of up to 300, which requires a resonance-based measurement for full accuracy. Unfortunately, a layout error discovered after fabrication produced too low capacitance due to missing overlap between the plates and the inductor. Hence, only the

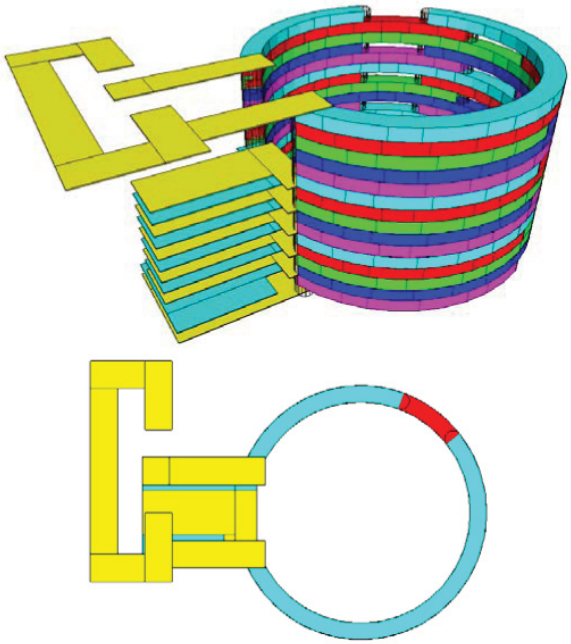

Fig. 16. Deep loop resonator.

basic S11 measurement of the inductor Q was possible for this structure. Qs of approximately 80 were measured with the network analyzer. As stated previously, an error as small as 1% in Γ could mean that the actual value is near the estimated value of 300 (see Fig. 8).

VI. Conclusion

3-D FTTF inductors embedded in LTCC have been shown to have Qs substantially higher than is possible with comparatively sized planar spirals. Measured values of 70 and above were confirmed by the use of multiple resonance-based and direct measurement techniques which help to overcome the accuracy limitations of VNAs in the application. These quality factors exceed that of the traditional spirals by a factor of approximately two.

Additionally, the 2-pole filter prototype demonstrates a possible application for the high-Q inductors. The filter has a measured selectivity Q of 20 using 40 mil inductors. Higher filter selectivity Q may be possible by using single turn inductors (like the one in the deep loop resonator) in place of solenoids. Future work is needed to develop these applications and to better understand the performance of FTTF inductors in general.

Acknowledgment

We would like to thank Honeywell FM&T as well as Sandia National Laboratories, Albuquerque, NM, for their support of this paper.

References

[1] W. B. Kuhn, X. He, and M. Mojarradi, "Modeling spiral inductors in SOS processes," *IEEE Trans. Electron Dev.*, vol. 51, no. 5, pp. 677–683, May 2004.

[2] N. M. Nguyen and R. G. Meyer, "Si IC-compatible inductors and LC passive filters," *IEEE J. Solid-State Circuits*, vol. 25, no. 4, pp. 1028–1031, Aug. 1990.

[3] K. C. Eun, Y. C. Lee, J. W. Lee, M. S. Song, and C. S. Park, "Fully embedded LTCC spiral inductors incorporating air cavity for high Q-factor and SRF," in *Proc. 54th Electron. Comp. Technol. Conf.*, vol. 1. Jun. 2004, pp. 1101–1103.
[4] A. Sutono, A. Pham, J. Laskar, and W. R. Smith, "Development of 3-D ceramic-based MCM inductors for hybrid RF/microwave applications," in *Proc. IEEE Symp. Rad. Freq. Integr. Circuits*, Anaheim, CA, Jun. 1999, pp. 175–178.
[5] K. A. Peterson, R. T. Knudson, E. J. Garcia, K. D. Patel, M. Okandan, C. K. Ho, C. D. James, S. B. Rohde, B. R. Rohrer, F. Smith, L. R. Zawicki, and B. D. Wroblewski, "LTCC in microelectronics, microsystems, and sensors," in *Proc. 15th Int. Conf. Mixed Design Integr. Circuits Syst.*, pp. 23–37, 2008.
[6] A. P. Boutz and W. B. Kuhn, "Measurement and potential performance of embedded LTCC inductors utilizing full tape thickness feature conductors," in *Proc. Ceramic Interconn. Ceramic Microsyst. Technol.*, 2009, pp. 259–264.
[7] W. B. Kuhn and N. M. Ibrahim, "Analysis of current crowding effects in multiturn spiral inductors," *IEEE Trans. Microw. Theory Tech.*, vol. 49, no. 1, pp. 31–38, Jan. 2001.
[8] J. Kita, A. Dziedzic, L. J. Golonka, and T. Zawada, "Laser treatment of LTCC for 3-D structures and elements fabrication," *Microelectron. Int.*, vol. 19, no. 3, pp. 14–18, 2002.
[9] H. A. Wheeler, "Simple inductance formulas for radio coils," *Proc. Inst. Rad. Eng.*, vol. 16, no. 10, pp. 1398–1400, Oct. 1928.
[10] P. F. Ryff, "Current distribution in helical solenoids," *IEEE Trans. Ind. Appl.*, vol. 8, no. 4, pp. 485–490, Jul. 1972.
[11] J. Aguilera, G. Matias, J. de No, A. Garcia-Alonso, and R. Berenguer, "A comparison among different setups for measuring on-wafer integrated inductors in RF applications," *IEEE Trans. Instrum. Meas.*, vol. 51, no. 3, pp. 487–491, Jun. 2002.
[12] W. B. Kuhn and A. P. Boutz, "Measuring and reporting high quality factors of inductors using vector network analyzers," *IEEE Trans. Microw. Theory Tech.*, vol. 58, no. 4, pp. 1046–1055, Apr. 2010.

Adam Paul Boutz received the B.S. and M.S. degrees in electrical engineering from Kansas State University, Manhattan, in 2007 and 2009, respectively.

He has been with Lockheed Martin Mission Systems and Sensors, Eagan, MN, where he is involved in the development of analog-optical data links.

William B. Kuhn (S'78–M'79–SM'97) received the B.S. degree from Virginia Polytechnic and State University (Virginia Tech), Blacksburg, in 1979, the M.S. degree from the Georgia Institute of Technology (Georgia Tech), Atlanta, in 1982, both in electrical engineering, and the Ph.D. degree from Virginia Tech in 1996.

He was with Ford Aerospace and Communications Corporation, Palo Alto, CA, from 1979 to 1981, designing satellite receiver equipment. From 1983 to 1992, he was with the Georgia Tech Research Institute, Atlanta, working on radar simulations and developing analog/digital circuit simulators and models. In 1996, he joined Kansas State University, Manhattan, as an Assistant Professor, and later became an Associate Professor in 2000 and Full Professor in 2006. He teaches courses in circuit design, communications theory, radio and microwave circuit/system design and very-large-scale integration. His current research interests include low-power radio electronics in complementary metal-oxide-semiconductor (CMOS), BiCMOS, GaAs and silicon on insulator technologies and have ranged from the characterization of spiral inductors to the design of radio receivers, transmitters and power amplifiers.

Dr. Kuhn received the Bradley Fellowship in 1993 from Virginia Tech and the Faculty Early Career Development (CAREER) Award from the National Science Foundation in 1999. He is also the recipient at Kansas State University of the Hollis Award for Excellence in Undergraduate Teaching in 2001, the Eta Kappa Nu Distinguished Faculty Award in 2002 and 2003, the Paslay Professorship in Electrical and Computer Engineering in 2004, and the Commerce Bank Award for excellence in undergraduate teaching in 2008.